The evaluation and calibration of fan-beam collimators

Jennifer L. Mahowald, Peter D. Robins, Michael K. O'Connor

Department of Radiology, Mayo Clinic, Rochester, MN 55905, USA

Abstract. The aims of this study were (a) to determine the true focal length of a fan-beam collimator and (b) to calibrate image size (mm/pixel) for each collimator to permit inter-comparison of image data acquired on different gamma camera systems. A total of six fan-beam collimators on three dual-head gamma camera systems were evaluated using a set of four cobalt-57 point source markers. The markers were arranged in a line in the transverse plane with a known separation between them. Tomographic images were obtained at three radii of rotation. From reconstructed transaxial images the distance between markers was measured in pixels and used to determine pixel size in mm/pixel. The system value for the focal length of the collimator was modified by up to ±100 mm and transaxial images were again reconstructed. To standardize pixel size between systems, the apparent radius of rotation during a single-photon emission tomography (SPET) acquisition was modified by changes to the effective collimator thickness. SPET images of a 3D brain phantom were acquired on each system and reconstructed using both the original and the modified values of collimator focal length and thickness. Co-registration and subtraction of the reconstructed transaxial images was used to evaluate the effects of changes in collimator parameters. Pixel size in the reconstructed image was found to be a function of both the radius of rotation and the focal length. At the correct focal length, pixel size was essentially independent of the radius of rotation. For all six collimators, true focal length differed from the original focal length by up to 26 mm. These differences in focal length resulted in up to 6% variation in pixel size between systems. Pixel size between the three systems was standardized by altering the value for collimator thickness. Subtraction of the co-registered SPET images of the 3D brain phantom was significantly improved after optimization of collimator parameters, with a 35%–50% reduction in the standard deviation of residual counts in the subtraction images. In conclusion, we have described a simple method for measurement of the focal length of a fan-beam collimator. This is an important parameter on multidetector systems for optimum image quality and where accurate co-registration of SPET to SPET and SPET to MRI studies is required.

Key words: Fan-beam collimator – Single-photon emission tomography – Quality control

Eur J Nucl Med (1999) 26:314–319

Correspondence to: M.K. O'Connor, Section of Nuclear Medicine, Charlton 2N-213, Mayo Clinic, Rochester, MN 55905, USA

Introduction

Fan-beam collimation was first described by Jaszczak et al. in 1979 [1]. The primary advantage of a fan-beam collimator is the 1.5- to 2-fold increase in sensitivity it affords over a parallel hole collimator of comparable resolution. Over the past 10 years fan-beam collimators have become widely available and are now used primarily in tomographic studies of the brain and heart. Despite their wide clinical use, no simple techniques exist that permit evaluation of the geometrical characteristics (focal length, collimator asymmetry) of fan-beam collimators. The reconstruction (rebinning) software uses collimator focal length in conjunction with the acquisition radius of rotation to correct for the magnifying effects of the collimator. An incorrect value for the focal length will change the true magnification factor for the image. Hence, collimator focal length directly affects the absolute size of the image pixel and consequently the mm/pixel calibration factor for the image. This can be important in a number of situations. For multidetector systems, uncorrected differences in the focal lengths of the fan-beam collimators will result in the summation of data sets of different sizes with consequent blurring of the tomographic data. If the single-photon emission tomography (SPET) data are to be co-registered with the patient's corresponding magnetic resonance (MR) study or SPET study acquired on a different system, errors in mm/pixel calibration factor will reduce the accuracy of the co-registered images.

The aims of this study were to describe a simple technique for the measurement of the focal length of a fan-beam collimator and to standardize tomographic pixel size between different gamma camera systems.

Materials and methods

We evaluated three sets of low-energy ultra-high-resolution fan-beam collimators designed for use on large-field-of-view dual-headed gamma camera systems. All collimators were of cast construction and were originally manufactured by Nuclear Fields (St. Mary's, NSW, Australia) for Elscint Inc. The collimators were installed on two Elscint Helix systems (systems 1 and 2) and one Elscint Varicam system (system 3) (Elscint, Inc., Haifa, Israel). All six collimators had a nominal focal distance from the focal line to the collimator surface of approximately 350 mm, with a field of view of 535 mm along the x-axis and 250 mm along the y-axis. Distance from the collimator surface to the surface of the crystal was 57 mm for all the collimators, giving an effective nominal focal length of 350+57=407 mm. Actual values for the collimator focal length were set by the manufacturer during installation and are listed in Table 1. A prerequisite for this study was the ability to modify the system file containing the fan-beam parameters. Figure 1 illustrates the four variables that could be set by the user in the system parameter file for each fan-beam collimator and the corresponding acquisition header file. The ability to edit the acquisition header file allowed us to reconstruct the same acquisition data set multiple times with different parameters.

For calibration of collimator focal length, a set of four cobalt-57 point source markers (1 mm active diameter, with approximately 3.7 MBq/source) were taped to a 15-cm-diameter plastic disk. The disk was placed in the headrest of the gamma camera so that the markers were perpendicular to the axis of rotation (±0.5°) and all lay in the same transaxial plane with a separation of 5 cm between markers. Markers were positioned with an accuracy of approximately 0.5 mm. Tomographic studies were acquired in a 128×128 word mode matrix over 360°. A total of 120 views were acquired at 3° intervals in step and shoot mode.

For each collimator three acquisitions were performed at different radii of rotation. The smallest radius of rotation was the minimum distance consistent with an unobstructed circular orbit around the markers and varied between systems due to differences in the size and shape of the head holders. The following radii of rotation were used: system 1: 9, 12, and 15 cm; system 2: 11.6, 12 and 15 cm; and system 3: 13, 15, and 18 cm. The radius of rotation is computed differently between systems 1/2 and system 3. For systems 1 and 2, it is computed as the distance from the center of rotation to the collimator surface, while on system 3 it is computed as the distance from the center of rotation to the surface of the crystal. For each acquisition the distances between the four markers (in centimeters) were noted.

All studies were reconstructed in an identical manner on an Elscint Xpert workstation (Version 5.1 software). A 1-pixel thick transaxial slice through the four markers was reconstructed using a standard filtered back-projection algorithm with a Metz filter [power = 3; full-width at half-maximum (FWHM) = 6 cm]. The value for the focal length of the fan-beam collimator (f+c, Fig. 1) was then modified (range = ±100 mm from nominal value) in the header information of the acquisition file and the planar data were again reconstructed as described above. From each transaxial image, the distances between the markers (in pixels) were measured by first obtaining linear profiles in both the x and y directions through each marker. The x and y location of the peak activity in each marker was obtained by the nearest neighboring technique [2], and the separation in pixels between markers was obtained by triangulation. From knowledge of the true distance between the markers, three mm/pixel factors were calculated for each transaxial image set and the mean value and coefficient of variation obtained. For each collimator, the relationship between the mm/pixel
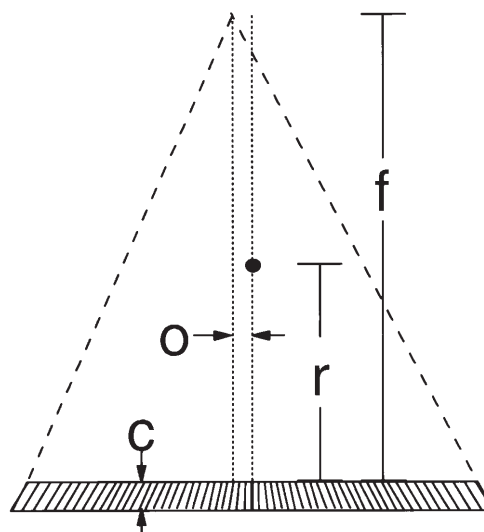
Fig. 1. Schematic diagram illustrating the various fan-beam collimator parameters that affect image size. These are: f, distance from focal line to collimator surface; c, collimator thickness; r, distance from center of rotation to collimator surface; and o, offset of focal line from center of rotation. For data reconstruction, collimator focal length = f+c, and radius of rotation = r+c

calibration factor and collimator focal length was plotted for the three studies acquired at different radii. Fourth-order polynomial fits were performed to the data points for each radius of rotation. The focal length corresponding to the cross-over point between the three fitted curves yields an identical mm/pixel factor for all three radii of rotation. The focal length at this cross-over point was then selected as the optimum focal length for that collimator in order to ensure that the mm/pixel calibration factor was independent of the radius of rotation.

The radius of rotation for a given acquisition comprises two factors: the thickness of the collimator and the distance between the collimator surface and the center of rotation (c and r respectively in Fig. 1). We examined the effect of changes in the radius of rotation on the mm/pixel calibration factor by changing the value for collimator thickness in the header file of the acquisition data set. The value for the radius of rotation was modified over the range ±10 mm while the focal length was set at the optimum value described above. The modified planar data were then reconstructed as described above.

To confirm the validity of the above technique for determination of collimator focal length, we performed tomographic acquisitions of a 3D volumetric brain phantom (Hoffman brain phantom, Data Spectrum Corp., Hillsborough, N.C.) on all three gamma camera systems. The phantom was filled with approximately 185 MBq of technetium-99m and was well agitated to ensure that the ^{99m}Tc was thoroughly mixed throughout the phantom. On each system, the phantom was positioned in the head holder and the radius of rotation set to that compatible with the smallest circular orbit around the phantom. Data were acquired in a 128×128 word mode matrix over 360° with 120 views. One-pixel-thick transaxial slices were reconstructed using a standard filtered back-projection algorithm with a Metz filter (power = 3; FWHM = 6 cm). The values for collimator focal length and thickness were then modified in the header files of each acquisition based on the results of the marker studies described above and the brain phantom studies were again reconstructed.

Following reconstruction, all transaxial data sets were exported in Interfile format to a UNIX workstation. On this workstation, a commercial image analysis software package (ANALYZE 7.5, Biomedical Imaging Resource, Mayo Foundation, Minn.) was utilized to compare the SPET images of the brain phantom acquired on the three systems. This software has been previously validated in both phantom and clinical studies [3], and was used to compare transaxial images between system 1 and system 2 and between system 1 and system 3, for both the default fan-beam parameters and the new parameters. The following processing steps were performed for each system to system comparison. In *step 1*, the two data sets were co-registered using a 3D surface matching algorithm [4]. This algorithm uses the mm/pixel calibration factor embedded in the image data to adjust for differences in pixel size between studies. In *step 2*, the co-registered data sets were normalized to the same total counts in the brain, with the median count in each study set to 100. In *step 3*, the normalized co-registered data sets were then subtracted on a slice by slice basis and the standard deviation of counts in the subtraction images was used to determine the accuracy of the registration process [3].

Results

Figure 2 plots the relationship between the mm/pixel calibration factor and the collimator focal length for the three radii of rotation. Results are shown for head 1 of system 1, which had a nominal focal length of 407 mm. Figure 2 indicates that the optimum value of the focal length is approximately 380 mm. At this focal length, image size is essentially independent of the acquisition radius of rotation. Similar results were obtained for the other five collimators. We found that for all six collimators, no unique cross-over point could be identified. The average of the three crossover points was used to determine the optimum collimator focal length. For the six collimators, Table 1 presents the default focal length, the focal lengths at the cross-over points, and the optimum focal length based on the average of the three cross-over points. The original mm/pixel calibration factor for each system was 2.2 mm/pixel. Table 2 presents the mm/pixel calibration factor for each collimator at the optimum focal length. The average value of the coefficients of variation from the three acquisitions was 1.33%. This error in the measurement of the mm/pixel calibration factor was due primarily to the error in determining the exact physical location of each marker.

For all three systems, there are slight differences between the calibration factors from head 1 and head 2. While these slight differences in image size (<2%) will have minimal impact on overall image quality, it is often desirable to adjust all heads to yield images of the same size. Fine adjustment of image size can be accomplished by changing the effective radius of rotation. As stated above, the radius of rotation comprises two components: a fixed component representing collimator thickness and a variable component that is determined by the acquisition geometry. Modifying the collimator thickness changes the effective radius of rotation. Figure 3A shows the effect of changes in the effective radius of rotation
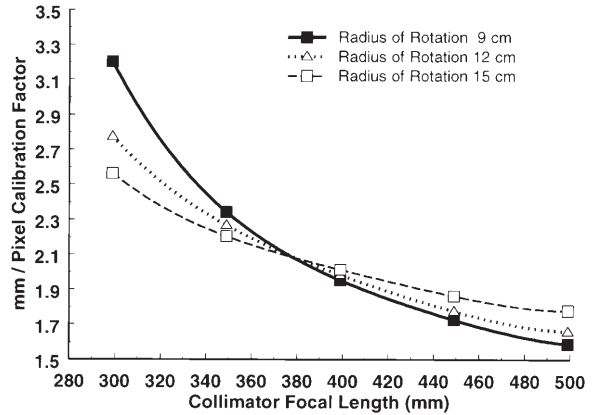
Fig. 2. Relationship between image size (mm/pixel calibration factor) and value for collimator focal length used in tomographic reconstruction, for studies acquired at three different radii of rotation. Results are shown for head 1, system 1 with a nominal collimator focal length of 407 mm

Table 1. Default and calculated focal lengths for the six fan-beam collimators

System	Default focal length (mm)	Calculated focal length (mm)	
		Average	Range
1: Head 1	399	380	377, 379, 382
1: Head 2	406	380	375, 381, 384
2: Head 1	402	402	400, 402, 403
2: Head 2	402	389	383, 385, 398
3: Head 1	398	423	415, 423, 430
3: Head 2	398	415	397, 417, 432

Table 2. Values of the mm/pixel calibration factors obtained using the calculated average collimator focal length, and standardized values of the mm/pixel calibration factors after adjustment of the collimator thickness

System	mm/pixel calibration factor		Adjustment in collimator thickness (mm)
	Calculated	Standardized	
1: Head 1	2.06	2.15	+9.2 mm
1: Head 2	2.11	2.15	+3.9 mm
2: Head 1	2.21	2.15	−5.2 mm
2: Head 2	2.21	2.15	−7.6 mm
3: Head 1	2.21	2.15	−6.5 mm
3: Head 2	2.27	2.15	−10.3 mm

on the mm/pixel calibration factor for head 1 on system 1. The results show that this factor is still dependent to a small degree on the radius of rotation, possibly due to the lack of a single cross-over point. Using the average value of the mm/pixel calibration factor for the three radii of rotation, Fig. 3B shows the comparable results for all six collimators. Hence with appropriate adjustments to the radii of rotation, it is possible to standardize the mm/pixel calibration factor between the three gamma
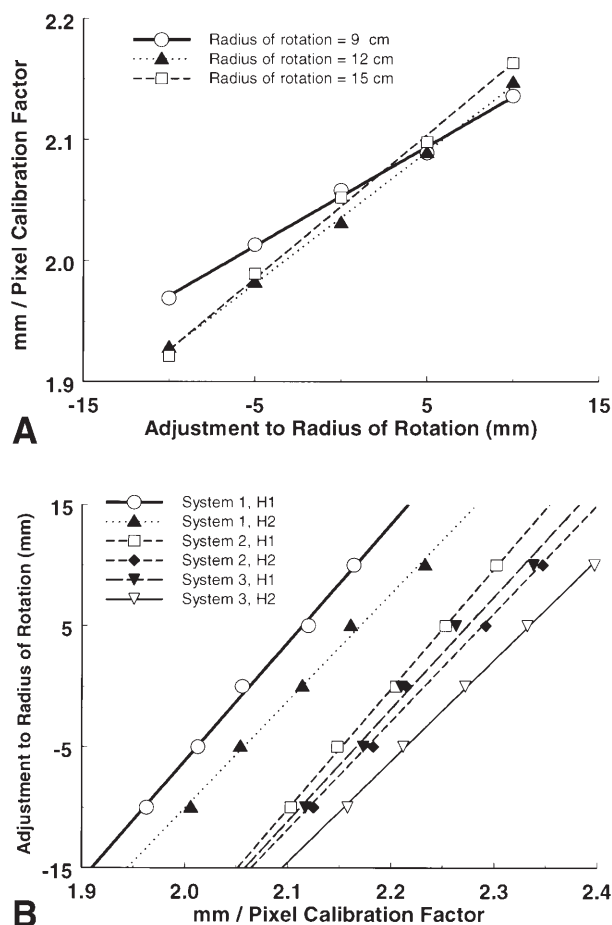
Fig. 3. A Effect of changes in the apparent system radius of rotation on image size (mm/pixel calibration factor) for studies acquired at three different radii of rotation on head 1 of system 1. **B** Adjustments to the radii of rotation required to obtain the same mm/pixel calibration factor on all six collimators

camera systems. Table 2 compares the calibration factors obtained with the cross-over point with those obtained after modification to the effective radius of rotation, together with the necessary change to the apparent collimator thickness. Identical calibration factors for all six collimators permit inter-comparison of images acquired on the three systems.

Figure 4 compares the co-registered images before and after adjustment of the collimator focal length and effective radius of rotation. With the default parameters the subtraction images showed a bright ring around the edges indicating a mismatch in image size (Fig. 4A). Re-analysis of the data sets using the optimal focal lengths and radii of rotation significantly reduced the magnitude of the mismatch between the images (Fig. 4B). However, there is still a subtle dark or bright rim around some of the images, indicating some residual mismatch. This may be due to the presence of a focal zone, rather than focal point, for each collimator, making it impossible to completely eliminate registration errors between images acquired on different systems. The standard deviation of counts in the subtracted images between system 1 and system 2 was reduced from 22.7 to 14.5, and that between system 1 and system 3 was reduced from 31.7 to 15.2. These results show that the new parameters significantly improved the correlation between image data acquired on the three systems. Figure 5 illustrates the effect of changes in collimator focal length on image size. Results are shown for system 3 using the default and calculated focal lengths.

On one collimator (head 1, system 3), it was noticed that the reconstructed point source images were semilunar in shape, consistent with the type of distortion expected from a center of rotation error. This may have been the result of asymmetry in the focal plane of the collimator. The application of a small center of rotation offset in the fan-beam parameter file for that collimator corrected this distortion.
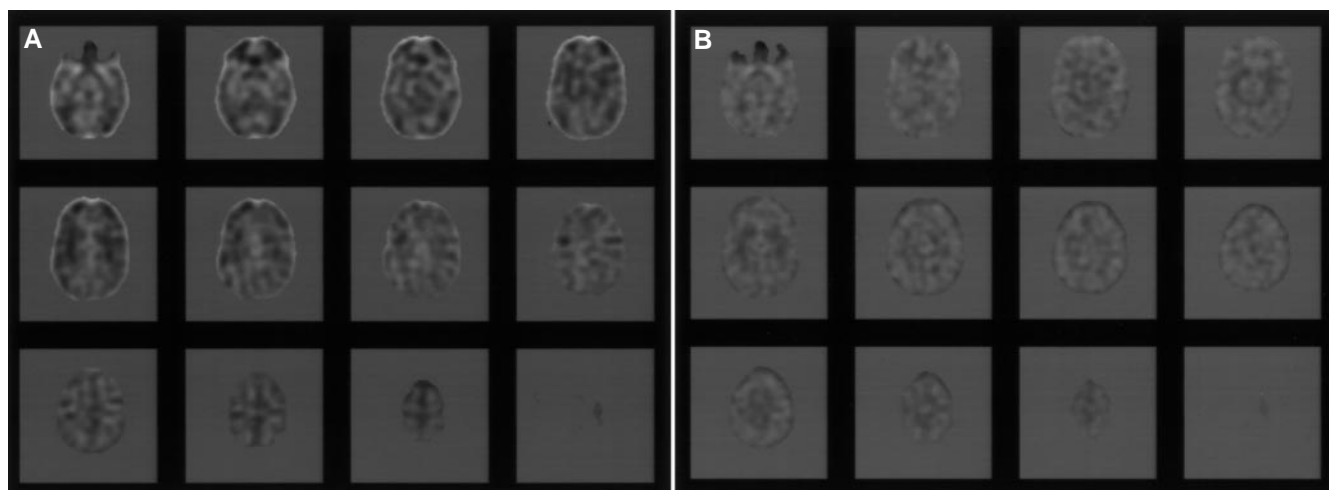
Fig. 4. Subtracted transaxial images of the brain from studies acquired on systems 1 and 2 using original fan-beam parameters (**A**) and optimized fan-beam parameters (**B**). Gray background represents zero counts. Bright and dark regions represent positive/negative differences between images
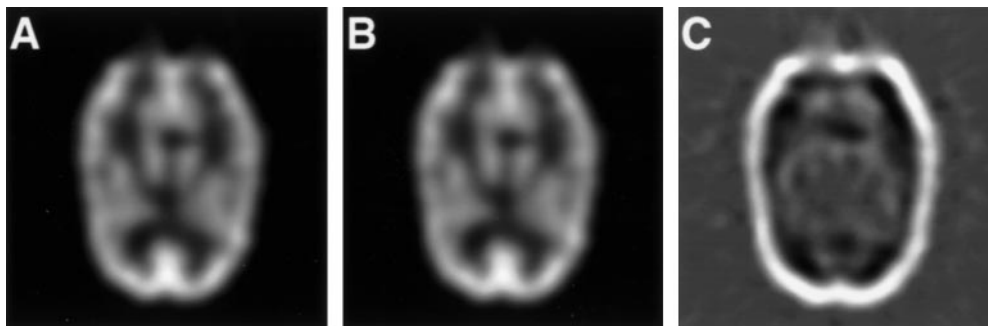
Fig. 5. Transaxial slice through the brain phantom obtained using default (**A**) and calculated (**B**) focal lengths for the fan-beam collimators on system 3. The effect of these minor changes in focal length on image size is shown in the subtraction image (**C**) (calculated-default). Gray background represents zero counts. Bright and dark regions represent positive/negative differences between images

Discussion

The gamma camera collimator is the most critical component of the imaging chain in terms of image quality. For tomographic imaging, an important aspect of the collimator is hole angulation. Variation in this parameter over the detector field of view leads to changes in the center of rotation and blurring of the reconstructed image data. While a number of studies have described techniques to measure collimator hole angulation [5, 6], none of these techniques are applicable to non-parallel hole collimators. For fan-beam and cone-beam collimators, hole angulation is intimately related to the focal length of the collimator, as variations in hole angle over the field of view will alter the focal point, essentially creating a focal zone. Increasing the deviation of hole angles from their correct values will increase the size of the focal zone. An estimate of collimator hole angulation in fan-beam or cone-beam collimators could be obtained from the evaluation of image uniformity from a line or point source placed at the focal line or focal point. However, this technique would require the development of software to quantitate the deviation of uniformity from that expected based on collimator characteristics. For fan-beam collimators, Liu et al. [7] have described a planar technique for estimation of collimator focal length based on trigonometrical analysis of the true versus measured location of a series of point sources placed at a fixed distance from the collimator face. This technique is in essence a variation of that described by Busemann-Sokole [5] for the evaluation of parallel and slant-hole collimators and relates variations in hole angle to changes in the collimator focal point. This technique does require accurate knowledge of the exact physical location of each point source relative to the crystal face. In this paper we have described a simple technique for accurate calculation of collimator focal length that can be used with any gamma camera system. The only prerequisite is access to the system parameter files that contain the various collimator-specific factors. The main disadvantage of the technique is that it does require multiple acquisitions and reconstruction of the data at different radii of rotation and collimator focal lengths. Fortunately, this process need only be performed once on each collimator to accurately characterize it.

With current manufacturing techniques there is a limit to the accuracy with which collimator hole angulation can be set. For parallel hole collimators, this value is typically ±0.25° and is likely to be larger for fan-beam and cone-beam collimators. Simple geometry shows that for a fan-beam collimator with a field of view of 535 mm and focal length of 350 mm, this variation in hole angulation will result in variations in focal length of ±3 mm at the edge of the field of view and ±5 mm midway between the center and edge of the field of view. In this context, the results in Table 1 are not unexpected and are consistent with the limitations of fan-beam technology. The results in Table 1 show that none of the six collimators had a single well-defined focal line, but came to a focal zone. These results are consistent with those of Liu et al. [7], who found variations (1 SD) of 8–26 mm in the focal line of fan-beam collimators. The presence of a focal zone rather than a focal line will alter image size as a function of the position of an object in the field of view. Consequently for a fixed object, this will result in changes in image size as a function of radius of rotation, even when the optimum focal length is used (Fig. 3). As shown in Fig. 4B, this makes it is difficult to accurately co-register images acquired with different fan-beam collimators.

On a single detector system, minor errors in collimator focal length have little impact on image quality. However, on multidetector systems, mismatch in focal length will result in the addition of images of different sizes. With the increasing use of co-registration techniques (SPET to MR and SPET to SPET) in brain imaging, accurate knowledge of image size is essential. With proper calibration of image size, the standard deviation of counts in the subtracted images was reduced to 14%–15%. These values can be compared with results previously reported from this laboratory using the same 3D brain phantom imaged a number of times on the same system with repositioning between studies [3]. Values for the standard deviation of 8%–10% were obtained in that study. While co-registration of images acquired on different systems is not as accurate as that obtained

from images acquired on the same system, it still resulted in a substantial improvement in the quality of the subtracted images (Fig. 4). Failure to account for differences in image size can lead not only to errors in the subtracted images, but also potentially to misregistration of functional and anatomical information.

In conclusion, we have described a simple technique for the evaluation of collimator focal length and the calibration of image size. Accurate knowledge of fan-beam collimator parameters is important in SPET to SPET and SPET to MR co-registration studies.

References

1. Jaszczak RJ, Chang LT, Murphy PH. Single-photon emission computed tomography using multislice fanbeam collimators. *IEEE Trans Nucl Sci* 1979; 26: 610–619.

2. NEMA. Performance measurements of scintillation cameras. National Electrical Manufacturers Association, 1994, Standards Publication No. NU-1. Washington, DC.

3. O'Brien TJ, O'Connor MK, Mullan BP, et al. Subtraction ictal SPET co-registered to MRI in partial epilepsy: description and technical validation of the method with phantom and patient studies. *Nucl Med Commun* 1998; 19: 31–45.

4. Jiang H, Robb RA, Holton KS. A new approach to three-dimensional registration of multimodality medical images by surface matching. In: Visualization in Biomedical Computing 1992. *Proc SPIE* 1992; 1808: 196–213.

5. Busemann-Sokole E. Measurement of collimator hole angulation and camera head tilt for slant and parallel hole collimators used in SPECT. *J Nucl Med* 1987; 28: 1592–1598.

6. Malmin RE, Stanley PC, Guth WR. Collimator angulation error and its effect on SPECT. *J Nucl Med* 1990; 31: 655–659.

7. Liu J, Loncaric S, Huang G, Chang W. The focussing quality of commercial fan-beam collimators. *J Nucl Med* 1996; 37: 207P.